Field-based Estimate of the Sediment Deficit in Coastal Louisiana

K. M. Sanks[1], J. B. Shaw[1], and K. Naithani[2]

[1]Department of Geoscience, University of Arkansas.

Kelly Sanks (kmsanks@uark.edu), John Shaw (shaw84@uark.edu)

[2]Department of Biological Sciences, University of Arkansas.

Kusum Naithani (kusum@uark.edu)

Corresponding author: Kelly Sanks (kmsanks@uark.edu)

Key Points:

- Field-based estimates of sediment deficit provide insight into changing deltaic conditions and are essential for restoration
- Accurate estimates of sediment deficit hinge on evaluating the coupled nature of sediment bulk density and subsidence rate at the same depth
- Organic accumulation accounts for ~30% of the recent sedimentation, contrasting with the Holocene stratigraphic record in coastal Louisiana

Abstract

Coastal and deltaic sediment balances are crucial for a region's sustainability. However, such balances remain difficult to quantify accurately, particularly for large regions. We calculate organic and mineral sediment mass and volume balances using field measurements from 273 Coastwide Reference Monitoring System sites across the Louisiana coast between 2006 and 2015. The rapid relative sea level rise rate (average 13.4 mm/yr) is offset by the small dry bulk densities observed (average 0.3 g/cm^3) to produce a 16.2 ± 41.1% mass deficit and 24.1 ± 14.0% volume deficit, significantly smaller than recent predictions for 2000 – 2100 (73 to 79% mass deficit). Geostatisical estimates show that this deficit is primarily located in areas not directly nourished by major rivers, yet these regions still accumulate ~24 MT/yr of mineral sediment. A fluvial sediment discharge of 113.8 MT/yr suggests a coast-wide trapping efficiency of 31.5 ± 15.8% of the riverine sediment, excluding subaqueous deposition. Organic accumulation accounts for 30% of all volume accumulation during our study period and total organic mass accumulation per unit area is relatively constant in both directly and indirectly nourished regions. Sediment characteristics in the modern coastal wetlands differ from the Holocene deposit, suggesting secular changes within the system that will likely continue to influence coastal dynamics over the coming decades. Our results suggest that the gap between accommodation and accumulation (mass or volume) during this decade was not as large as the previously predicted century average.

1 Introduction

Coastal wetlands are economically and environmentally important regions of high biodiversity. They help mitigate the detrimental impacts of storms (Cahoon et al., 2006; Shepard et al., 2011), are important global sinks for carbon (Hopkinson et al., 2012), and provide a source of livelihood for millions of people (Gramling & Hagelman, 2005). Globally, deltas and their coastal wetlands have been deteriorating, as historic management practices have altered the sediment budget and rising relative sea level has increased accommodation (Coleman et al., 2008; Couvillion et al., 2017; Day et al., 2000; Stanley, 1996; Teatini et al., 2011; Wang et al., 2012). Despite these stressors, recent work has shown that many deltas are currently prograding (Besset et al., 2019; Nienhuis et al., 2020; Ninfo et al., 2018) though we lack a systematic understanding of this shift.

Over the past century, about 5,000 km^2 of Louisiana's coastal wetlands have transitioned to open water environments (Couvillion et al., 2017). Historic management practices have caused significant changes to the distribution of sediment across the coast, which has in turn changed wetland characteristics (Cahoon, 1994; Day et al., 2011). The predicted loss of much of the remaining 16,200 km^2 of Louisiana wetlands has prompted recent government efforts to focus on the restoration and protection of these valuable ecosystems (Blum & Roberts, 2012; Colten, 2016). Despite current net land loss on the Mississippi River Delta (Couvillion et al., 2017) and the fact that it has been thoroughly studied (Paola et al., 2011), the coastal sediment balance remains poorly quantified. This presents an important gap in sustainability monitoring.

A sediment deficit is defined as the difference between the mass or volume of accumulating sediment and the mass or volume needed to fill the accommodation created by relative sea level rise (RSLR). Land loss from the last century in coastal Louisiana suggests such a sediment deficit. It was previously modeled for 2000 – 2100 to be 73 – 79% (Table S1), predicting the inevitable drowning of a significant portion of the remaining coastal wetlands by 2100 (Blum & Roberts, 2009, hereafter defined as BR09). This model was based on five key assumptions. First, the sediment mass accumulation rate was assumed to be 40% of the sediment discharge of the Mississippi and Atchafalaya rivers (trapping efficiency, *TE*). Second, the deposit was assumed to have a sediment bulk density (ρ) of 1.5 g/cm^3 (43% porosity). Third, the subsidence rates were assumed to range from 3 – 8 mm/yr (6 – 12 mm/yr RSLR). Fourth, no mineral sediment input to wetlands isolated from rivers by artificial levees was assumed for the period 2000 – 2020. Finally, organic sediment mass accumulation was not considered. Aspects of the deposit were assumed from measurements of the Holocene Mississippi Delta and compared to modern RSLR and sediment transport measurements.

The sediment balance is the primary control on long-term delta evolution, so precise constraints are essential for successful implementation of coastal restoration and management plans (Bentley et al., 2014; Paola et al., 2011). In this study, we use the Louisiana Coastwide Reference Monitoring System (CRMS) to calculate the first field-based estimate of sediment mass and volume balance in coastal Louisiana. The CRMS dataset is compiled by the United States Geological Survey (USGS) and the Louisiana Coastal Protection and Restoration Authority (CPRA). This distributed set of monitoring stations (Figure 1) provide direct measurements of sediment accretion and estimates of shallow subsidence rates between 2006 and 2015 (the study period), as well as sediment characteristics derived from 24-cm-deep cores taken during site installation, which began in 2006 (Folse et al., 2008). By assuming that sediment characteristics during the study period were similar to those measured in the shallow core, a synoptic sediment balance can be geostatistically interpolated across the domain (Diggle & Ribeiro, 2007). We assess the variability between directly nourished areas (the areas fed by the Mississippi and Atchafalaya Rivers) and indirectly nourished areas (which have no significant riverine sediment input). We then show the first regional estimate of wetland sediment trapping efficiency by combining sediment mass accumulation with direct discharge and suspended sediment concentration data from two USGS river gauging stations. Finally, we estimate organic mass accumulation in the remaining 16, 200 km^2 of coastal wetlands in the domain.

2 Methods

2.1 Data Collection

Sediment mass and volume accumulation rates (spatially integrated measurements of sediment deposition, i.e. tonne/km^2/yr [mass] and m^3/yr [volume]) were geostatistically modeled from point measurements of sediment characteristics, including vertical accretion rate (V_a; cm/yr). Sediment characteristics for each CRMS site were collected for 391 sites along the coast at the time of site establishment, which began in 2006. Each CRMS site includes a shallow core for sediment characteristics (bulk density [ρ; g/cm^3] and organic fraction [F_{org}; -]), surface elevation change measurements, and vertical accretion monitoring via marker horizons (Folse et al., 2008).

Organic fraction is calculated from loss on ignition. Since F_{org} are average values derived from shallow sediment cores (24 cm deep), decomposition that occurs from the surface to 24 cm depth is included in total organic accumulation estimates (see results section 3.3). We assume that the average ρ and F_{org} of this material is characteristic of the material that accumulated on the surface after site establishment.

The CRMS monitoring also captures vertical sediment accretion and erosion in coastal wetlands using cryogenic coring when the sediment erosion is small enough that the feldspar horizon is not destroyed (Folse et al., 2008). Thus, the dataset does not account for subaqueous deposition and/or erosion, wetland edge erosion, or substantial erosion of the wetland interior (see discussion section 4.3). V_a is measured by sediment accretion on the marker horizon. Shallow compaction is calculated by subtracting surface elevation change from V_a.

A subset of 274 sites as described in prior work by Jankowski et al. (2017) are selected for interpolation of sediment characteristics; however, one site was omitted from our study, as this site did not contain sediment characteristics (n = 273 for this study; Figure 1). The subset for V_a rates were chosen based on three parameters: (1) the sites were never re-established because of damage, (2) the sites have at least one continuous V_a record, and (3) the accretion record is at least 6 years long. Linear regressions of all V_a measurements, taken approximately every 6 months after site establishment, were calculated to obtain an average V_a for each of the 273 sites (Jankowski et al., 2017).

2.2 Interpolation and Statistical Analysis

We use Bayesian kriging for creating maps of V_a, ρ, and F_{org} using a 1-km^2 grid covering the extent of the study domain (Figure 2). We chose Bayesian kriging because it integrates data and model to predict unobserved values, produces uncertainty estimates of the prediction, and is less likely to be biased by parameter choices (such as semivariogram nugget and range) as compared to the traditional approaches (e.g. ordinary kriging) (Diggle & Ribeiro, 2007). We used uniformed priors and allowed the model to sample from a large parameter space. To meet the normality assumptions, we transformed the variables (Figure S3) using the boxcox transformation embedded within Bayesian kriging in geoR package (Ribeiro, 2018). We then used the Sharpiro-Wilks test to confirm normality of the transformed variables.

Although microtopography in marshes is likely to reflect somewhat different sediment characteristics (Stribling et al., 2007), we are unable to directly characterize changing conditions between CRMS stations. Further, the dataset is not able to capture changes in wetland characteristics that may occur between CRMS sites that are separated by old distributary levees or other hydrologic boundaries. However, we incorporate the 1st order spatial trends into our model, which show that F_{org}, ρ, and V_a do not have constant means across the coast, thus, variability in sediment properties is considered in the model. Preliminary work showed that ordinary kriging under-estimated the sediment deficit because of these spatial trends and that Bayesian kriging, with a 1st order trend, removed spatial biases. We used leave-one-out cross-validation to validate the results of Bayesian kriging (Figure S5). The cross-validation results show a good agreement between field-data and predictions (V_a $r^2 = 0.96$, ρ $r^2 = 0.88$, and F_{org} $r^2 = 0.86$). For all model parameters and analysis code, please refer to the Supporting Information.

Preliminary work also showed that sediment balances were sensitive to the land area considered. Hence, we choose a conservative estimate of coastal wetland area (16,554 km^2) from 2013 provided by the USGS (Sasser et al., 2014). The kriged maps were clipped to include only data that falls within the ten CPRA coastal hydrologic basins (16,176 km^2; Figure 1). The shapefile was created in the summer of 2013 using aerial imagery to map vegetation along the Louisiana coast in order to analyze wetland change. These wetlands include brackish, salt, fresh, and inland swamp ecosystems with CRMS sites spanning the entire study area (Figure 1). We chose this shapefile specifically because it excludes cities, rivers, areas of high elevation, and levees (Nienhuis et al., 2017). Further, it is the most recent land/water polygon for the coast, so we assume areas that drowned before our study period are removed.

We estimate the amount of sediment accumulating in the wetlands during the study period by converting interpolated sediment properties, ρ and V_a, to total sediment mass and volume accumulation rates (see Appendix B; Equations B1 and B7). We also calculated mineral and organic mass and volume accumulation rates (Equations B2, B3, B8, and B9). We estimate the mass and volume balance over the study domain (Equations B17 and B27) by comparing the amount (mass or volume) of sediment needed to fill accommodation created by RSLR each year (Equations B15 and B25) to the mass or volume accumulation rates. We compare the deficit in the directly and indirectly nourished regions, as well as the ten different hydrologic basins along the coast to understand the spatial relationship.

In order to do this, we multiplied the clipped interpolated raster maps (V_a, F_{org}, and ρ) to create a map of sediment mass accumulation rate at each pixel (sum of all pixels = total mass accumulation rate) in ArcGIS. The extracted data, including interpolated data and error for each grid square, was exported as a csv file. We use calculated covariances (σ; Table S2) during error propagation since the variables are all correlated (Figure S2). In particular, ρ (g/cm^3) and F_{org} (-) are very strongly negatively correlated (in log space), as can be seen from an r^2 value of 0.87 and a very low p-value of $2.69 * 10^{-124}$ (Figure S2b).

We used CRMS subsidence rates originating from shallow compaction of Holocene sediments combined with deep subsidence originating from GPS data (Karegar et al., 2015) for calculation of accommodation. We calculate independent spatial statistics for subsidence rates and see that the nugget for the semivariogram of subsidence rates is 0.43 cm/yr and the range is 0 km. The range is slightly different than, but comparable to, the 5 km range calculated by Nienhuis et al. (2017). The range shows the distance between points in which the data is spatially autocorrelated. Since there is no spatial autocorrelation (0 km range), we use the weighted average subsidence rate to estimate total accommodation along the coast (Figure S6). For this same reason, we use average subsidence rates for each basin in the analysis of the sediment budget at the basin scale. These rates are quite variable along the coast, but the weighted mean subsidence rate is 10.4 ± 0.86 mm/yr.

The global mean eustatic SLR rate measured using altimetry has been shown to be 3.0 ± 0.4 mm/yr (Nerem et al., 2018), potentially approaching 3.5 mm/yr (WCRP Global Sea Level Budget Group, 2018). A more regional study shows a SLR rate of 2.0 ± 0.4 mm/yr on the Louisiana coast (Letetrel et al., 2015). We use the global mean eustatic SLR rate for our study (3.0 ± 0.4 mm/yr), which gives a total RSLR rate of 13.4 ± 0.9 mm/yr.

We calculate a combined sediment discharge from the Mississippi (at Belle Chasse, LA, USGS Station: 07374525) and Atchafalaya (at Melville, LA, USGS Station: 07381495) rivers for the study period. We use trapezoidal integration, which assumes linear change from one measurement to the next, to calculate total suspended sediment concentration, water discharge and sediment discharge for both rivers. The integration gives a total sediment discharge of 113.8 MT/yr over the 10-year period (Figure S1). We use this sediment discharge to calculate the coast wide trapping efficiency (Equation B13).

3 Results

3.1 Coastal Louisiana Sediment Deficit

The total mass needed to fill the 16,176 km^2 of coastal wetlands that existed in 2013 (Couvillion et al., 2017) at a rate of 13.4 ± 0.9 mm/yr and at an average ρ of 0.29 g/cm^3 is 57.5 ± 16.0 MT/yr (one standard error). Our geostatistical analysis estimates that 48.2 ± 17.2 MT/yr of sediment mass accumulated over the study period. Of this, 35.9 ± 18.0 MT/yr was mineral sediment and 12.3 ± 5.11 MT/yr was organic material (Figure 3). This results in a 9.34 ± 23.5

MT/yr or 16.2 ± 41.1% mass deficit along the coast. If we neglect the organic contribution, the total mass deficit would be 37.6 ± 43.1%. Further, if mean sea level along the Louisiana coast was 2.0 mm/yr (the regional average), then the sediment mass deficit would have been 9.50 ± 42.9% (5.06 ± 22.8 MT/yr) (tabulated in Supporting Information). The combined fluvial (Mississippi River and Atchafalaya River) sediment discharge during the study period was 113.8 MT/yr (Figure S1). Comparison of this mineral river sediment discharge to mineral mass accumulation yields a *TE* of 31.5% ± 15.8%.

The sediment volume balance along the coast differs from the mass balance because mass accumulation (ρV_a) and accretion are nonlinearly related due to weak correlation between ρ and V_a (Figure S2c). Using the same area and RSLR, the volume needed to fill the accommodation is 218 x 10^6 ± 14.8 x 10^6 m^3/yr. A total volume of 165 x 10^6 ± 26.4 x 10^6 m^3/yr of sediment accumulated along the coast during the study period. 115 x 10^6 ± 26.4 x 10^6 m^3/yr was mineral sediment, while 50.4 x 10^6 ± 0.229 x 10^6 m^3/yr was organic sediment. This results in a 52.3 x 10^6 ± 30.2 x 10^6 m^3/yr or 24.1 ± 14.0% sediment volume deficit, slightly larger than the mass deficit, but with far less uncertainty. If we neglect organic contribution to the volume of sediment accumulated, the deficit would be 47.2 ± 14.3%.

3.2 Basin Analysis

We perform a sediment budget analysis (Figure 4, all estimates tabulated in Supporting Information) for the entire domain using the ten different hydrologic basins (see Figure 1 for locations). We consider the Mississippi River Delta, Atchafalaya Basin, and Breton Sound to be the directly nourished basins. We consider Breton Sound a directly nourished basin, as it receives fluvial sediment from the Mississippi River during high floods (Smith et al., 2015). Further, it was directly nourished during the 2008 high flow event, which occurred during our 10-year study period (Allison & Meselhe, 2010).

A spatial trend is observed in sediment characteristics (ρ, F_{org}, and V_a) across the coast (Figure 2). The western region of the coast has lower V_a than the eastern region, beginning at the Atchafalaya basin. This trend is due to the location of the sediment input sources (Mississippi and Atchafalaya rivers), which cause ρ to be higher and F_{org} to be lower in areas located near a river. The indirectly nourished areas receive mineral sediment either from elsewhere in the wetland, shallow bays, or the continental shelf (sediment nourishment from minor rivers, the Davis Pond (Keogh et al., 2019) diversion, and the Caernarvon diversion are neglected). Even though lower ρ produces larger sediment volumes for a given sediment mass, the indirectly nourished areas still have about 15% more sediment deficit by mass and 10% by volume (Figure 4, tabulated in Supporting Information).

Total, mineral, and organic accumulation rates also vary across the delta (Figure 3; Supporting Information). The main distinction is the varying mass accumulation rates in directly nourished areas compared to indirectly nourished areas (p-value = 0.053; see Figure 1 for locations). The western portion of the coast has lower total, mineral, and organic sediment mass accumulation rates, while the eastern region has higher total and organic sediment mass accumulation rates. Interestingly, the middle portion of the coast, between Atchafalaya and Barataria basins, has large organic mass accumulation rates, relative to the rest of the study area. This organic mass accumulation helps offset the lower mineral sediment mass accumulation rates, allowing this region to have an average total sediment mass accumulation rate.

3.3 Organic Material Accumulation

Over the study period, 123 ± 16.2 MT of organic material accumulated within the domain. 19.8 ± 3.31 MT accumulated in the directly nourished areas, while 104 ± 13.3 MT accumulated in the indirectly nourished areas. However, the directly and indirectly nourished areas sequester similar amounts of organic material per unit area each year (918 ± 485 and 739 ± 300 tonne/km^2/yr, respectively). Higher fraction of organic material in a wetland tends to correlate with a wetland that has a higher fraction sediment mass deficit (Figure 6).

4 Discussion

The CRMS dataset allows us to statistically model the first regional-scale, field-based estimate of sediment mass and volume accumulation and corresponding deficit within the coastal Louisiana wetlands, accounting for changes in environmental conditions observed in recent years. Our conservative estimates show that between 2006 and 2015, there was not enough sediment (measured by mass or volume) accumulating in coastal wetlands to keep pace with RSLR. However, a sediment mass surplus during this period cannot be ruled out, due to large uncertainty related to the incorporation of ρ when calculating mass balance estimates.

4.1 A New Estimate of Sediment Deficit

It is useful to compare our estimates to previous estimates from BR09, even though the study area and riverine sediment discharge cannot be compared explicitly. Our sediment deficit considers the entire Louisiana coast, while BR09 only considered the relatively sediment-rich Mississippi Delta region. Using the updated post-dam sediment load (Supporting Information 1.2), BR09 predicted average mass deficits of 129 to 187 MT/yr (73 – 79% for 2000-2100; Table S1). Remarkably, our sediment mass deficit (9.34 ± 23.5 MT/yr) is far smaller than the sediment deficit previously estimated by BR09. We discuss the reasons for this discrepancy below.

For simplicity, BR09 neglected organic accumulation in the deposit. This may have been justified by the predominantly clastic deposits of the Holocene, but core surveys show peat forming environments have increased (Hijma et al., 2017). We show that the sediment accumulated is 25.5% organic material by mass and 30.5% by volume in current deltaic conditions. Coastal wetlands that are starved of mineral sediment are thought to become more organic-rich (Bohacs & Suter, 1997; Kosters et al., 1987), and we show that organic fraction increases with increasing sediment deficit (Figure 6). However, organic mass accumulation per unit area remains roughly constant in directly and indirectly nourished areas (918 vs. 739 tonne/km^2/yr; section 3.4), similar to recent work by Holmquist et al. (2018). If we neglect organic accumulation, our results suggest that the small sediment deficit would increase to a 38% mass deficit or a 47% volume deficit. Thus, organic deposits should not be neglected when calculating sediment deficits in the Mississippi Delta or global coastal wetlands (Kirwan & Megonigal, 2013; Reed, 2002; Ye et al., 2015).

Our work uses substantially different estimates of deposit bulk density and subsidence rate than BR09. The shallow cores at the CRMS stations show a mean dry bulk density of 0.29 g/cm^3, corresponding to a 90% porosity, assuming a mineral sediment density of 2.65 g/cm^3. In contrast, BR09 assumed a dry bulk density of 1.5 g/cm^3, which corresponds to a 45% porosity. Thus, the dry bulk densities near the surface of coastal wetlands, including those on the bird's foot (Mississippi River Delta hydrologic basin), are much smaller than bulk densities estimated from buried Holocene strata. If using the same sediment load and *TE*, a lower bulk density leads to the accumulation of more volume. A reduction of the assumed dry bulk density from 1.5 g/cm^3 to 1.0 g/cm^3 (for example) would reduce the BR09 sediment deficit calculated by 33%. Hence, field-based estimates of bulk density are inherently necessary for accurate estimates of sediment deficit in deltas worldwide.

Relatedly, our total subsidence rate (average 10.4 ± 0.83 mm/yr) is higher than the 3 – 8 mm/yr used by BR09. Subsidence on the Louisiana Coast is primarily due to shallow sediment compaction, meaning that ρ and subsidence rates are highly coupled properties that both decrease nonlinearly with depth (Keogh & Törnqvist, 2019; Törnqvist et al., 2006). Therefore, one must compare the subsidence rate and ρ at the same horizon in order to accurately estimate the sediment needed. The CRMS data is particularly valuable because it provides measurements of subsidence at the wetland surface and ρ in the top 24 cm of soil. Therefore, the small bulk densities and high subsidence rates found at the surface are appropriate to compare directly and significantly offset one another when calculating coastal sediment deficits, both in Louisiana and worldwide.

Finally, BR09 assumed zero sediment input to the Mississippi Delta wetlands from 2000 – 2020, as levees prevent the flow of water and sediment to the wetland interior. However, we show that a substantial amount of mineral sediment accumulated (~36 MT/yr) in the wetlands from 2006 – 2015. Despite artificial levees that prevent sediment transport from rivers to wetlands, other mechanisms must support mineral sediment transport and subsequent deposition in these wetlands (see discussion section 4.3).

It is important to note that deltas worldwide, including coastal Louisiana, have experienced many secular changes over the last century, including hydrologic basins becoming indirectly nourished, accelerated eustatic sea level rise and significant coastal wetland loss. These changes have likely altered the spatial distribution of bulk densities, subsidence rates, and organic fractions. The stability of the delta top in the future depends on changes to these highly coupled marsh characteristics. Hence, we conclude that the sediment deficits we document here may only persist for a short time (decades?) if further secular changes occur. Improved meso-scale modeling of coastal sediment deficits will need to incorporate these feedbacks to improve sustainability forecasts for coastal Louisiana or other large deltas.

The utility of interpolated sediment deficits can be also seen by comparing our sediment deficit to CMRS averaged statistics from Jankowski et al. (2017; J17). Without spatial interpolation, J17 found the mean vertical accretion rate (10.7 mm/yr) to be around 11% smaller than their estimate of RSLR (12.0 mm/yr). The interpolated average accretion rate is 10.2 mm/yr is 15% smaller than their estimate of RSLR. Similarly, J17 estimate a 20% volume deficit using our value of RSLR (13.4 ± 0.9 mm/yr), whereas we predict a 24% volume deficit. While of the same order, this comparison shows that geostatistical modeling of wetland characteristics can improve estimates of sediment deficits by ~4% (~2 MT/yr) relative to the extensive CRMS network alone, furthering the goal of monitoring coastal sustainability.

4.2 Limitations

The CRMS network monitors accretion on wetland platforms and cannot characterize several types of erosion and deposition in coastal wetlands, including wetland edge erosion, significant wetland platform erosion, and subaqueous deposition. Wetland erosion at the edges of ponds results in lateral changes in wetland extent. The CRMS stations measure V_a change to wetland platforms and are not designed to measure any lateral erosion of wetland edges. Over 34 years, there has been 250 km^2 of marsh edge erosion (Ortiz et al., 2017). If the depth of this marsh erosion is 2 m (Wilson & Allison, 2008) and the sediment has an average ρ of 1.15 g/cm^3 (Bomer et al., 2019), this would result in about 17 MT/yr of edge erosion over the 34-yr period, which is small in relation to mass accumulation on the wetland platform.

Accretion rates (V_a) would be biased if wetland platform (vertical) erosion is not accounted for. However, we show this potential limitation does not affect our study period (Smith et al., 2015). In many cases, accretion time series at the CRMS sites showed short periods of erosion (thickness reduction) within the long-term depositional signal. Hence, we consider the deposition rates to be characteristic of decadal scale wetland stability. We also rule out the possibility that some of the CRMS sites were neglected because erosion removed an accretion record. 118 sites were not used during our analysis (see methods section 2.2), but none of these sites showed removal of feldspar plots due to erosion that was greater than accretion. Therefore, we assume delta top erosion (i.e. large storm events) is captured within the short-term erosion signals observed at the CRMS sites and does not bias V_a.

The CRMS sites also do not measure delta front deposition, which is significant in parts of the bird's foot (MRD hydrologic basin), as well as the Wax Lake and Atchafalaya deltas in Atchafalaya Bay. There has been about 3 m of sediment deposited over 100 km^2 on the Wax Lake Delta (WLD) between 1974 and 2016 (Shaw et al., 2018). Assuming an average ρ for delta front sediments (24 cm – 3 m depth) of 1.77 g/cm^3 (33% porosity) (Shields et al., 2017, Supporting Information), the sediment mass accumulation is equivalent to about 12.6 MT/yr since formation. The deposition on the Atchafalaya Delta and the bird's foot of the Mississippi River Delta is estimated to be about 5 times larger than on the WLD, as the WLD receives about 1/6th of the combined (Mississippi and Atchafalaya rivers) fluvial discharge (Kim et al., 2009). We estimate that these three areas accumulate roughly 76 MT of sediment each year. This results in subaqueous deposition rates that are around 157% of the wetland mass accumulation rates (48.2 MT/yr). Though unaccounted for in our analysis (and weakly constrained here), this subaqueous deposition appears to be an important component of the coastal sediment balance.

4.3 Field Based Estimate of Wetland Trapping Efficiency

BR09 estimate a 40% *TE* in the Mississippi River Delta over the Holocene Epoch using a 450 MT/yr fluvial sediment discharge, whereas we estimate a 28% *TE* for a similar region (hydrologic basins: Atchafalaya, Terrebonne, Barataria, 'birds foot', Breton Sound, Ponchartrain, and Pearl) over the past decade using a 113.8 MT/yr sediment discharge. Interestingly, the *TE* assumed by BR09 is in line with our results, even at vastly different timescales and fluvial sediment discharge. The reduced sediment discharge is potentially due to natural variability of fluvial sediment transport or may be a part of the trend of reduced sediment transport since 1970 (Blum & Roberts, 2009; Mize et al., 2018).

A primary driver of the loss of deltaic marshes in the 20th century is the reduced sediment supply to the marsh platform, as artificial levees cut off riverine sediment supply (Gagliano et al., 1981). We see that just 11% of the mineral sediment delivered by the major rivers is trapped in areas that are directly nourished. The 'birds foot' has a TE = 5.47 ± 2.00% and the Atchafalaya has a TE = 9.85 ± 4.02% (tabulated in Supporting Information). These estimates are in line with previous estimates of 5 – 30% for the Wax Lake Delta (a directly nourished region located within the Atchafalaya basin) (Esposito et al., 2017). Comparatively, 24.4 MT/yr of mineral sediment accumulates in indirectly nourished wetlands, which constitutes 24% of the riverine sediment transported past the directly nourished regions (Equation B13). The higher *TE* estimated in the indirectly nourished areas is mostly due to the larger area, but also due to the lower estimated sediment supply. We see that the directly nourished areas accumulate about 3 times the amount of mineral sediment per unit area compared to indirectly nourished areas.

Sediment produced from marsh edge erosion has been shown to accumulate back on the marsh platform (Hopkinson et al., 2018). This mineral sediment derived from edge erosion (~17 MT/yr, section 4.2) is likely accounted for in the CRMS accretion rates as it gets redistributed; therefore, the total trapping efficiency could be as low as 17%.

We find it remarkable that significant mineral sediment mass accumulates in indirectly nourished areas. We argue the mineral sediment mass that accumulates in indirectly nourished wetlands each year is delivered through tides or storms (derived from the continental shelf) or from somewhere else on the marsh platform (Roberts et al., 2015; Stumpf, 1983). Continental shelf sediment dynamics will influence the indirect *TE* as well. The discovery of sediment starvation on the proximal continental shelf (Maloney et al., 2018) and frequent resuspension events (Obelcz et al., 2018) are both consistent with the export of continental shelf muds into indirectly nourished basins. If there was no mineral sediment deposited in the indirectly nourished wetlands, the sediment deficit would be 76%. Although the indirectly nourished areas do not trap enough mineral sediment to keep pace with RSLR, the mineral sediment transport process, though poorly understood, is crucial for the sustainability of these regions.

4.4 Implications for coastal restoration

Volume and mass estimates are both necessary when creating coastwide restoration plans. While there is only a small sediment mass deficit along the coast (16%), there is a slightly larger volume deficit from 2006 – 2015 (24%). The slight positive correlation between ρ and V_a (Figure S2) explains the lower sediment mass deficit because sediment surplus regions, such as the Mississippi River 'bird's foot', have accretion that is both more rapid and more dense than the delta wide average. If a controlled diversion could divert surplus sediment to indirectly nourished regions and the sediment deposits at a lower bulk density (with all other relationships steady), the volume deficit could be substantially reduced.

Relatedly, the sediment deficit could potentially be mitigated by increasing *TE*. Since the total *TE* is only about 32% (11% in the directly nourished areas and 24% of the remainder in the indirectly nourished areas), management strategies should focus on ways of trapping a portion of the remaining 70% of sediment along the coast through optimal diversion of sediment through sheltered diversion sites (e.g. Esposito et al., 2017). A relationship (or lack thereof) between *TE* and changes in fluvial sediment discharge would have a first order effect on sediment deficit, but such a relationship is unclear if continental shelf sediment sources can somewhat offset fluvial sediment discharge. Ultimately, the relatively low sediment deficit between 2006 and 2015 provides a more optimistic short-term outlook for the system than previous estimates suggest. A comprehensive understanding of the recent sediment deficit in progradational deltas will help further our understanding of these complex systems. Since small sediment deficits (as shown here) will likely affect land area change and other key coastal processes over coastal planning and management timescales, further work understanding this landscape response timescale will increase the effectiveness of these management goals.

5 Conclusion

Sustaining the remaining 16,200 km^2 of wetlands in coastal Louisiana is of extreme importance. Successful restoration plans hinge on accurate estimates of the sediment deficit. Using the Coastwide Reference Monitoring System, we calculate the first field-based estimate of sediment deficit in coastal Louisiana. Our analysis shows that between 2006 and 2015, coastal Louisiana had a sediment mass deficit of ~15% and a volume deficit of ~25%. This is a smaller sediment deficit (by mass and volume) than previous estimates for two important reasons. First, small bulk densities found in the surface sediments significantly offset large subsidence rates. Second, organic material makes up about 30% of the volume of these surface sediments and is extremely important in sustaining the current coastal land area. Although the sediment properties seen in the modern wetlands may be a disequilibrium response to changing conditions, they seem nearly sufficient for maintaining wetlands over decadal timescales.

Directly nourished regions trap 11% of riverine sediment, have above-average bulk densities and accretion rates, and have a small organic fraction. In contrast, indirectly nourished regions have small bulk densities and accretion rates, but high organic fraction. Even so, indirectly nourished regions accumulate substantial amounts of mineral sediment derived from local or continental shelf sources, equivalent of a 24% trapping efficiency. These properties offset one another to make organic accumulation rates vary by only 20% across the system.

Our analysis poses new challenges to simple mass balance models of delta sustainability. The coupling between wetland properties (e.g. bulk density, organic fraction, etc.), sediment trapping, and changing boundary conditions (sea level rise, coastal management) make modeling of secular changes to the system (such as wetland area) a daunting task. This difficulty makes data driven estimates of deltaic sediment deficits even more important. Our work suggests a present day, system-scale deficit in coastal Louisiana that is less dire than previously thought.

Acknowledgments, Samples, and Data

We would like to thank all the reviewers, especially Dr. Torbjörn Törnqvist, whose insight helped greatly improve our manuscript. We would also like to thank Dr. Aaron Shew for his contribution to the geostatistical analysis. The University of Arkansas (Fayetteville) Graduate School and the Department of Geoscience funded this project. K.M.S. led the study. J.B.S. advised the study. K.N. contributed to the geostatistical analyses. K.M.S. wrote the manuscript with contributions from J.B.S and K.N. There are no financial interests of the authors that might be perceived as being a conflict of interest.

Data and materials availability:

(1) CRMS Data was collected by the LCPRA and USGS. These data can be found in the supplementary materials of Jankowski (2017) or on the online CRMS database (https://www.lacoast.gov/crms_viewer2/Default.aspx).
(2) The USGS collected sediment concentration and water discharge data, and these data are found online at https://waterdata.usgs.gov/nwis.
(3) Interpolation data and code are published online in a data repository in compliance with the FAIR data project guidelines (DOI: 10.6084/m9.figshare.11663748).

References

Allison, M., & Meselhe, E. (2010). The use of large water and sediment diversion in the lower Mississippi River (Louisiana) for coastal restoration. *Journal of Hydrology*, *387*, 346–360. https://doi.org/10.1016/j.jhydrol.2010.04.001

Bentley, S. J., Freeman, A. M., Willson, C. S., Cable, J. E., & Giosan, L. (2014). Using What We Have: Optimizing Sediment Management in Mississippi River Delta Restoration to Improve the Economic Viability of the Nation | SpringerLink. In *Perspectives on the Restoration of the Mississippi Delta* (pp. 85–97). Dordrecht: Springer Berlin Heidelberg. Retrieved from https://link.springer.com/chapter/10.1007/978-94-017-8733-8_6

Besset, M., Anthony, E. J., & Bouchette, F. (2019). Multi-decadal variations in delta shorelines and their relationship to river sediment supply: An assessment and review. *Earth-Science Reviews*, *193*, 199–219. https://doi.org/10.1016/j.earscirev.2019.04.018

Blum, M. D., & Roberts, H. H. (2009). Drowning of the Mississippi Delta due to insufficient sediment supply and global sea-level rise. *Nature Geoscience*, *2*(7), 488–491. https://doi.org/10.1038/ngeo553

Blum, M. D., & Roberts, H. H. (2012). The Mississippi Delta Region: Past, Present, and Future. *Annual Review of Earth and Planetary Sciences*, *40*(1), 655–683. https://doi.org/10.1146/annurev-earth-042711-105248

Bohacs, K., & Suter, J. (1997). Sequence stratigraphic distribution of coaly rocks: Fundamental controls and paralic examples. *American Association of Petroleum Geologists Bulletin*, *81*(10), 28.

Bomer, E. J., Bentley, S. J., Hughes, J. E. T., Wilson, C. A., Crawford, F., & Xu, K. (2019). Deltaic morphodynamics and stratigraphic evolution of Middle Barataria Bay and Middle Breton Sound regions, Louisiana, USA: Implications for river-sediment diversions. *Estuarine Coastal and Shelf Science*, *224*, 20–33. https://doi.org/10.1016/j.ecss.2019.03.017

Cahoon, D. R. (1994). Recent Accretion in Two Managed Marsh Impoundments in Coastal Louisiana. *Ecological Applications*, *4*(1), 166–176. https://doi.org/10.2307/1942126

Cahoon, D. R., Hensel, P. F., Spencer, T., Reed, D. J., McKee, K. L., & Saintilan, N. (2006). Coastal Wetland Vulnerability to Relative Sea-Level Rise: Wetland Elevation Trends and Process Controls. In J. T. A. Verhoeven, B. Beltman, R. Bobbink, & D. F. Whigham (Eds.), *Wetlands and Natural Resource Management* (Vol. 190, pp. 271–292). Springer Berlin Heidelberg. https://doi.org/10.1007/978-3-540-33187-2_12

Coleman, J. M., Huh, O. K., & Braud, D. (2008). Wetland Loss in World Deltas. *Journal of Coastal Research*, (24 (10024)), 1–14. https://doi.org/10.2112/05-0607.1

Colten, C. E. (2016). Environmental Management in Coastal Louisiana: A Historical Review. *Journal of Coastal Research*, 699–711. https://doi.org/10.2112/JCOASTRES-D-16-00008.1

Couvillion, B. R., Beck, H., Schoolmaster, D., & Fischer, M. (2017). *Land area change in coastal Louisiana (1932 to 2016)* (No. 3381). U.S. Geological Survey. https://doi.org/10.3133/sim3381

Day, J. W., Britsch, L. D., Hawes, S. R., Shaffer, G. P., Reed, D. J., & Cahoon, D. (2000). Pattern and process of land loss in the Mississippi Delta: A Spatial and temporal analysis of wetland habitat change. *Estuaries*, *23*(4), 425–438. https://doi.org/10.2307/1353136

Day, J. W., Kemp, G. P., Reed, D. J., Cahoon, D. R., Boumans, R. M., Suhayda, J. M., & Gambrell, R. (2011). Vegetation death and rapid loss of surface elevation in two contrasting Mississippi delta salt marshes: The role of sedimentation, autocompaction and sea-level rise. *Ecological Engineering*, *37*(2), 229–240. https://doi.org/10.1016/j.ecoleng.2010.11.021

Diggle, P. J., & Ribeiro, P. J. (2007). *Model-based Geostatistics*. Springer Berlin Heidelberg.

Esposito, C. R., Shen, Z., Törnqvist, T. E., Marshak, J., & White, C. (2017). Efficient retention of mud drives land building on the Mississippi Delta plain. *Earth Surface Dynamics*, *5*(3), 387–397. https://doi.org/10.5194/esurf-5-387-2017

Folse, T. M., Sharp, L. A., West, J. L., Hymel, M. K., Troutman, J. P., McGinnis, T. E., et al. (2008). *A Standard Operating Procedures Manual for the Coastwide Reference Monitoring System-Wetlands: Methods for Site Establishment, Data Collection, and Quality Assurance/Quality Control* (p. 228). Baton Rouge, LA: Louisiana Coastal Protection and Restoration Authority.

Gagliano, S. M., Meyer-Arendt, K. J., & Wicker, K. M. (1981). Land Loss in the Mississippi River Deltaic Plain, *31*. Retrieved from http://archives.datapages.com/data/gcags/data/031/031001/0295.htm

Gramling, R., & Hagelman, R. (2005). A Working Coast: People in the Louisiana Wetlands. *Journal of Coastal Research*, 112–133.

Hopkinson, C. S., Cai, W.-J., & Hu, X. (2012). Carbon sequestration in wetland dominated coastal systems—a global sink of rapidly diminishing magnitude. *Current Opinion in Environmental Sustainability*, *4*(2), 186–194. https://doi.org/10.1016/j.cosust.2012.03.005

Hopkinson, C. S., Morris, J. T., Fagherazzi, S., Wollheim, W. M., & Raymond, P. A. (2018). Lateral Marsh Edge Erosion as a Source of Sediments for Vertical Marsh Accretion. *Journal of Geophysical Research: Biogeosciences*, *123*(8), 2444–2465. https://doi.org/10.1029/2017JG004358

Jankowski, K. L., Törnqvist, T. E., & Fernandes, A. M. (2017). Vulnerability of Louisiana's coastal wetlands to present-day rates of relative sea-level rise. *Nature Communications; London*, *8*, 14792. http://0-dx.doi.org.library.uark.edu/10.1038/ncomms14792

Karegar, M. A., Dixon, T. H., & Malservisi, R. (2015). A three-dimensional surface velocity field for the Mississippi Delta: Implications for coastal restoration and flood potential. *Geology*, *43*(6), 519–522. https://doi.org/10.1130/G36598.1

Keogh, M. E., & Törnqvist, T. E. (2019). Measuring rates of present-day relative sea-level rise in low-elevation coastal zones: a critical evaluation. *Ocean Science*, *15*(1), 61–73. https://doi.org/10.5194/os-15-61-2019

Keogh, M. E., Kolker, A. S., Snedden, G. A., & Renfro, A. A. (2019). Hydrodynamic controls on sediment retention in an emerging diversion-fed delta. *Geomorphology*, *332*, 100–111. https://doi.org/10.1016/j.geomorph.2019.02.008

Kim, W., Mohrig, D., Twilley, R., Paola, C., & Parker, G. (2009). Is It Feasible to Build New Land in the Mississippi River Delta? *Eos, Transactions American Geophysical Union*, *90*(42), 373–374. https://doi.org/10.1029/2009EO420001

Kirwan, M. L., & Megonigal, J. P. (2013). Tidal wetland stability in the face of human impacts and sea-level rise. *Nature*, *504*(7478), 53–60. https://doi.org/10.1038/nature12856

Kosters, E. C., Chmura, G. L., & Bailey, A. (1987). Sedimentary and botanical factors influencing peat accumulation in the Mississippi Delta. *Journal of the Geological Society*, *144*(3), 423–434. https://doi.org/10.1144/gsjgs.144.3.0423

Letetrel, C., Karpytchev, M., Bouin, M.-N., Marcos, M., SantamarÍa-Gómez, A., & Wöppelmann, G. (2015). Estimation of vertical land movement rates along the coasts of the Gulf of Mexico over the past decades. *Continental Shelf Research*, *111*, 42–51. https://doi.org/10.1016/j.csr.2015.10.018

Mize, S. V., Murphy, J. C., Diehl, T. H., & Demcheck, D. K. (2018). Suspended-sediment concentrations and loads in the lower Mississippi and Atchafalaya rivers decreased by half between 1980 and 2015. *Journal of Hydrology*, *564*, 1–11. https://doi.org/10.1016/j.jhydrol.2018.05.068

Nerem, R. S., Beckley, B. D., Fasullo, J. T., Hamlington, B. D., Masters, D., & Mitchum, G. T. (2018). Climate-change–driven accelerated sea-level rise detected in the altimeter era. *Proceedings of the National Academy of Sciences*, *115*(9), 2022–2025. https://doi.org/10.1073/pnas.1717312115

Nienhuis, J. H., Ashton, A. D., Edmonds, D. A., Hoitink, A. J. F., Kettner, A. J., Rowland, J. C., & Törnqvist, T. E. (2020). Global-scale human impact on delta morphology has led to net land area gain. *Nature*, *577*(7791), 514–518. https://doi.org/10.1038/s41586-019-1905-9

Nienhuis, Jaap H, Törnqvist, T. E., Jankowski, K. L., & Keogh, M. E. (2017). A New Subsidence Map for Coastal Louisiana. *GSA Today*. https://doi.org/10.1130/GSATG337GW

Ninfo, A., Ciavola, P., & Billi, P. (2018). The Po Delta is restarting progradation: geomorphological evolution based on a 47-years Earth Observation dataset. *Scientific Reports*, *8*. https://doi.org/10.1038/s41598-018-21928-3

Obelcz, J., Xu, K., Bentley, S. J., O'Connor, M., & Miner, M. D. (2018). Mud-capped dredge pits: An experiment of opportunity for characterizing cohesive sediment transport and slope stability in the northern Gulf of Mexico. *Estuarine, Coastal and Shelf Science*, *208*, 161–169. https://doi.org/10.1016/j.ecss.2018.04.039

Ortiz, A. C., Roy, S., & Edmonds, D. A. (2017). Land loss by pond expansion on the Mississippi River Delta Plain. *Geophysical Research Letters*, *44*(8), 2017GL073079. https://doi.org/10.1002/2017GL073079

Paola, C., Twilley, R. R., Edmonds, D. A., Kim, W., Mohrig, D., Parker, G., et al. (2011). Natural processes in delta restoration: application to the Mississippi Delta. *Annual Review of Marine Science*, *3*, 67–91. https://doi.org/10.1146/annurev-marine-120709-142856

Reed, D. J. (2002). Sea-level rise and coastal marsh sustainability: geological and ecological factors in the Mississippi delta plain. *Geomorphology*, *48*(1), 233–243. https://doi.org/10.1016/S0169-555X(02)00183-6

Ribeiro, P. J. (2018, July 29). geoR package | R Documentation. Retrieved June 28, 2019, from https://www.rdocumentation.org/packages/geoR/versions/1.7-5.2.1

Roberts, H. H., DeLaune, R. D., White, J. R., Li, C., Sasser, C. E., Braud, D., et al. (2015). Floods and Cold Front Passages: Impacts on Coastal Marshes in a River Diversion Setting (Wax Lake Delta Area, Louisiana). *Journal of Coastal Research*, *31*(5), 1057–1068. https://doi.org/10.2112/JCOASTRES-D-14-00173.1

Sasser, C. E., Visser, J. M., Mouton, E., Linscombe, J., & Hartley, S. B. (2014). *Vegetation Types in Coastal Louisiana in 2013* (Scientific Investigations Map).

Shaw, J. B., Estep, J. D., Whaling, A. R., Sanks, K. M., & Edmonds, D. A. (2018). Measuring subaqueous progradation of the Wax Lake Delta with a model of flow direction divergence. *Earth Surface Dynamics*, *6*(4), 1155–1168. https://doi.org/10.5194/esurf-6-1155-2018

Shepard, C. C., Crain, C. M., & Beck, M. W. (2011). The Protective Role of Coastal Marshes: A Systematic Review and Meta-analysis. *PLOS ONE*, *6*(11), e27374. https://doi.org/10.1371/journal.pone.0027374

Shields, M. R., Bianchi, T. S., Mohrig, D., Hutchings, J. A., Kenney, W. F., Kolker, A. S., & Curtis, J. H. (2017). Carbon storage in the Mississippi River delta enhanced by environmental engineering. *Nature Geoscience*, *10*(11), 846–851. https://doi.org/10.1038/ngeo3044

Smith, J. E., Bentley, S. J., Snedden, G. A., & White, C. (2015). What Role do Hurricanes Play in Sediment Delivery to Subsiding River Deltas? *Scientific Reports*, *5*(1). https://doi.org/10.1038/srep17582

Stanley, D. J. (1996). Nile delta: extreme case of sediment entrapment on a delta plain and consequent coastal land loss. *Marine Geology*, *129*(3), 189–195. https://doi.org/10.1016/0025-3227(96)83344-5

Stribling, J., Cornwell, J., & Glahn, O. (2007). Microtopography in tidal marshes: Ecosystem engineering by vegetation? *Estuaries and Coasts*, *30*, 1007–1015. https://doi.org/10.1007/BF02841391

Stumpf, R. P. (1983). The process of sedimentation on the surface of a salt marsh. *Estuarine, Coastal and Shelf Science*, *17*(5), 495–508. https://doi.org/10.1016/0272-7714(83)90002-1

Teatini, P., Tosi, L., & Strozzi, T. (2011). Quantitative evidence that compaction of Holocene sediments drives the present land subsidence of the Po Delta, Italy. *Journal of Geophysical Research: Solid Earth*, *116*(B8). https://doi.org/10.1029/2010JB008122

Törnqvist, T. E., Bick, S. J., Borg, K. van der, & Jong, A. F. M. de. (2006). How stable is the Mississippi Delta? *Geology*, *34*(8), 697–700. https://doi.org/10.1130/G22624.1

Wang, M., Qi, S., & Zhang, X. (2012). Wetland loss and degradation in the Yellow River Delta, Shandong Province of China. *Environmental Earth Sciences*, *67*(1), 185–188. https://doi.org/10.1007/s12665-011-1491-0

WCRP Global Sea Level Budget Group. (2018). Global sea-level budget 1993–present. *Earth System Science Data*, *10*(3), 1551–1590. https://doi.org/10.5194/essd-10-1551-2018

Wilson, C., & Allison, M. (2008). An equilibrium profile model for retreating marsh shorelines in southeast Louisiana. *Estuarine Coastal and Shelf Science - ESTUAR COAST SHELF SCI*, *80*, 483–494. https://doi.org/10.1016/j.ecss.2008.09.004

Ye, S., Laws, E. A., Yuknis, N., Ding, X., Yuan, H., Zhao, G., et al. (2015). Carbon Sequestration and Soil Accretion in Coastal Wetland Communities of the Yellow River Delta and Liaohe Delta, China. *Estuaries and Coasts*, *38*(6), 1885–1897. https://doi.org/10.1007/s12237-014-9927-x

Figure 1. Coastal Louisiana study area.

The shapefile used for analysis (16,176 km^2 area) is outlined in black. The black dots represent the subset of 273 Coastwide Reference Monitoring System (CRMS) sites used in this study. The directly nourished basins are outlined in red (bird's foot, Breton Sound, and Atchafalaya), and the rest of the coast is indirectly nourished. The ten hydrologic basins, defined by the Coastal Protection and Restoration Authority (CPRA), that are used for the sediment budget basin analysis are shaded in various colors (see legend).

Figure 2. Interpolated accretion rates, bulk density, and organic fraction.

*Interpolated maps of **(a)** accretion rate **(b)** bulk density and **(c)** organic fraction were created using Bayesian kriging.*

Figure 3. Total, Mineral, and Organic Sediment Accumulation Rate along the Louisiana Coast.

*Interpolated maps of **(a)** total mass accumulation rate, **(b)** mineral sediment mass accumulation rate, and **(c)** organic sediment mass accumulation rate in coastal Louisiana. The western Chenier Plain has much lower total, mineral, and organic sediment mass accumulation rates, even though this region has higher fraction organic matter than the directly nourished areas. The directly nourished areas are accumulating almost enough sediment to fill the accommodation, as denoted by the tan-blue colors in these areas. The high organic accumulation rates in Atchafalaya basin help offset the sediment deficit.*

Figure 4. Sediment Accumulation in Coastal Louisiana Hydrologic Basins.

The total sediment mass accumulation rate for each coastal Louisiana basin, represented from west to east along the x-axis. Total (blue bar), organic (green bar), and mineral (grey bar) sediment mass accumulation rate for each basin along the coast. The black dots represent the area normalized sediment mass accumulation rate for each basin. For locations of basins, please refer to figure 1.

Figure 5. Sediment Deficit per Area.

The sediment mass deficit of most basins overlaps with zero. A few indirectly nourished basins have significant sediment mass deficits per area (Calcasieu/Sabine, Mermentau, and Pearl Basins).

Figure 6. Percent Organic Material vs. Percent Sediment Deficit.

The percent sediment mass deficit is positively correlated with the percent organic material present. Higher fraction organic material in a marsh is indicative of a larger sediment deficit in the marsh. Further, the indirectly nourished areas (yellow) tend to have larger sediment mass deficits, as well as more organic material than the directly nourished areas (blue). The total *coastal land area is shown as a black x. The solid black regression line shows the linear regression between fraction total mass deficit (points on figure) and fraction organic material, while the dashed line shows the linear regression between the fraction mineral mass deficit and fraction organic material.*

Appendix A- Variables

$\rho_i - sediment\ density\ at\ pixel\ i\ (\frac{g}{cm^3})$

$V_{a_i} - vertical\ accretion\ rate\ at\ pixel\ i\ (\frac{cm}{yr})$

$F_{org_i} - fraction\ organic\ matter\ at\ pixel\ i\ (-)$

$A\ - coastal\ Louisiana\ study\ area; 16{,}176\ km^2$

$m_T - total\ mass\ of\ sediment\ accumulated\ each\ year\ (\frac{MT}{yr})$

$m_{org} - total\ \ mass\ of\ organic\ sediment\ accumulated\ each\ year\ (\frac{MT}{yr})$

$m_m - total\ mass\ of\ mineral\ sediment\ accumulated\ each\ year\ (\frac{MT}{yr})$

$\delta_{\rho_i} - standard\ deviation\ of\ bulk\ density\ at\ pixel\ i\ (\frac{g}{cm^3})$

$\delta_{V_{a_i}} - standard\ deviation\ of\ vertical\ accretion\ rate\ at\ pixel\ i\ (\frac{cm}{yr})$

$\delta_{F_{org_i}} - standard\ deviation\ of\ fraction\ organic\ matter\ at\ pixel\ i\ (-)$

$\sigma_{V\rho} - covariance\ between\ bulk\ density\ and\ vertical\ accretion\ rate\ at\ pixel\ i$

$\sigma_{\rho F} - covariance\ between\ bulk\ density\ and\ fraction\ organic\ matter\ at\ pixel\ i$

σ_{VF}
$- covariance\ between\ fraction\ organic\ matter\ and\ vertical\ accretion\ rate\ at\ pixel\ i$

$\delta_{m_T} - the\ error\ on\ the\ total\ sediment\ mass\ accumulation\ rate\ (\frac{MT}{yr})$

$\delta_{m_{org}} - the\ error\ on\ the\ organic\ sediment\ mass\ accumulation\ rate\ (\frac{MT}{yr})$

$\delta_{m_m} - the\ error\ on\ the\ mineral\ sediment\ mass\ accumulation\ rate\ (\frac{MT}{yr})$

$V_T - total\ volume\ accumulation\ rate\ (\frac{m^3}{yr})$

$V_{org} - organic\ volume\ deficit\ rate\ (\frac{m^3}{yr})$

$V_m - mineral\ volume\ deficit\ rate\ (\frac{m^3}{yr})$

$\delta_{v_T} - error\ of\ the\ total\ sediment\ volume\ accumulation\ rate\ (\frac{m^3}{yr})$

$\delta_{v_{org}} - error\ of\ the\ organic\ sediment\ volume\ accumulation\ rate\ (\frac{m^3}{yr})$

$\delta_{v_m} - error\ of\ the\ mineral\ sediment\ volume\ accumulation\ rate\ (\frac{m^3}{yr})$

$Q_s - riverine\ sediment\ discharge\ (\frac{MT}{yr})$

$SSC - suspended\ sediment\ concentration\ (\frac{mg}{L})$

$Q_w - riverine\ water\ discahrge\ (\frac{MT}{yr})$

$m_{Rm} - mineral\ mass\ accumulation\ rate\ in\ directly\ nourished\ areas\ (\frac{MT}{yr})$

$TE - trapping\ efficiency\ (-)$

$\delta TE - error\ of\ trapping\ efficiency\ (-)$

$RSLR_i - relative\ sea\ level\ rise\ rate\ at\ pixel\ i\ (\frac{cm}{yr})$

$\delta_{RSLR_i} - error\ of\ relative\ sea\ level\ rise\ rate\ at\ pixel\ i\ (0.1\frac{cm}{yr})$

$m_N - total\ sediment\ mass\ accumulation\ rate\ needed\ to\ sustain\ land\ area\ (\frac{MT}{yr})$

$\delta_{m_N} - error\ of\ sediment\ mass\ accumulation\ rate\ needed\ to\ sustain\ land\ area\ (\frac{MT}{yr})$

$m_D - sediment\ mass\ deficit\ (\frac{MT}{yr})$

$\delta_{m_D} - error\ of\ sediment\ mass\ deficit\ (\frac{MT}{yr})$

$F_{m_D} - fraction\ mass\ deficit\ (-)$

$\delta_{F_{m_D}} - error\ of\ fraction\ mass\ deficit\ (-)$

$F_{m_{Dm}} - fraction\ mineral\ mass\ deficit\ (-)$

$m_{DA} - sediment\ deficit\ normalized\ by\ area\ (\frac{tonne}{km^2 yr})$

$\delta_{m_{DA}} - error\ of\ sediment\ deficit\ normalzied\ by\ area\ (\frac{tonne}{km^2 yr})$

$m_{D_m} - sediment\ mass\ deficit\ without\ organic\ accumulation\ (\frac{MT}{yr})$

$\delta_{m_{D_m}} - error\ of\ sediment\ mass\ deficit\ without\ organic\ accumulation\ (\frac{MT}{yr})$

$V_N - sediment\ volume\ needed\ to\ sustain\ current\ land\ area\ (\frac{m^3}{yr})$

$\delta_{V_N} - error\ of\ sediment\ volume\ needed\ to\ sustain\ current\ land\ area\ (\frac{m^3}{yr})$

$V_D - sediment\ volume\ deficit\ (\frac{m^3}{yr})$

$\delta_{V_D} - error\ of\ sediment\ volume\ deficit\ (\frac{m^3}{yr})$

$F_{V_D} - fraction\ volume\ deficit\ (-)$

$\delta_{F_{V_D}} - error\ of\ fraction\ volume\ deficit\ (-)$

$V_{D_m} - sediment\ volume\ deficit\ without\ organics\ (\frac{m^3}{yr})$

$\delta_{V_{D_m}} - error\ of\ sediment\ volume\ deficit\ without\ organics\ (\frac{m^3}{yr})$

$F_{m_{org}} - total\ fraction\ organic\ material\ \ by\ mass\ (-)$

$\delta_{F_{m_{org}}} - error\ of\ total\ fraction\ organic\ material\ \ by\ mass\ (-)$

$F_{V_{org}} - total\ fraction\ organic\ material\ by\ volume\ (-)$

$\delta_{F_{V_{org}}} - error\ of\ total\ fraction\ organic\ material\ \ by\ volume\ (-)$

Appendix B- Equations

To calculate an estimate for total (mineral plus organic) sediment mass accumulation rate in the Mississippi Delta wetlands (m_T), the following equation was used:

$$m_T = A \sum_{i \in A} \rho_i V_{a_i} , \qquad (B1)$$

where m_T is the total sediment mass accumulation rate in Mississippi Delta wetlands (MT/yr), V_{a_i} is vertical accretion rate (cm/yr) at an individual grid cell (i) within the coastal Louisiana wetland area (A; ~16176 km^2 – area of shapefile), and ρ_i is dry bulk density (g/cm^3) at an individual pixel. We applied the same methods to calculate the organic mass accumulation rate (m_{org}; MT/yr):

$$m_{org} = A \sum_{i \in A} \rho_i V_{a_i} F_{org_i} , \qquad (B2)$$

where F_{org_i} is fraction organic matter at an individual grid cell (-). Total mineral sediment mass accumulation rate (m_m; MT/yr) was then calculated using:

$$m_m = m_T - m_{org}. \tag{B3}$$

We further differentiated between areas fed by the Mississippi and Atchafalaya Rivers (directly nourished) and the rest of the coast, which we assume to be indirectly nourished. The same analysis was then conducted on a shapefile excluding the Mississippi River, Breton Sound, and Atchafalaya Basins. These new mineral and organic sediment mass accumulation rates are assumed to be areas of indirect nourishment. These numbers were then subtracted from total, mineral, and organic sediment mass accumulation rates to determine a sediment mass accumulation rate of areas that are directly nourished. Lastly, we used the same equations to calculate mass accumulation for the 10 different hydrologic basins within the study domain.

We propagate error for the sediment mass accumulation rate using the standard error of V_a, ρ, and F_{org} and linear propagation. We also considered spatial autocorrelation, but we found it to be small because the range of the semivariogram was small (~ 25 to 40 km for V_a, ρ, and F_{org}; Figure S4, Table S2) relative to the width of the study domain (400 km). The error for mass accumulation rates were calculated as follows:

$$\delta_{m_T} = m_T \sum_{i\in A} \sqrt{\left(\frac{\delta_{V_{a_i}}}{V_{a_i}}\right)^2 + \left(\frac{\delta\rho_i}{\rho_i}\right)^2 + \left(2V_{a_i}\rho_i\sigma_{V\rho}\right)} \;\;, \tag{B4}$$

$$\delta_{m_{org}} = m_{org} \sum_{i\in A} \sqrt{\left(\frac{\delta_{V_{a_i}}}{V_{a_i}}\right)^2 + \left(\frac{\delta\rho_i}{\rho_i}\right)^2 + \left(\frac{\delta_{F_{org_i}}}{F_{org_i}}\right)^2 + \left(2(V_{a_i}\rho_i\sigma_{V\rho} + V_{a_i}F_{org_i}\,\sigma_{VF} + \rho_i F_{org_i}\,\sigma_{\rho F})\right)}\,, \tag{B5}$$

$$\delta_{m_m} = \sqrt{\left(\delta_{m_T}\right)^2 + \left(\delta_{m_{org}}\right)^2}\,, \tag{B6}$$

where δ_{m_x} is the total interpolation error (MT/yr) for total, organic, and mineral sediment mass accumulation rate along the coast, δ_{ρ_i} is the estimated standard deviation of dry bulk density for each grid cell (g/cm^3), $\delta_{V_{a_i}}$ is the estimated standard deviation of vertical accretion rate for each grid cell (cm/yr), and $\delta_{F_{org_i}}$ is the estimated standard deviation of fraction organic matter (-) for each grid cell. σ is the covariance number between two variables (Table S2).

We calculate total sediment volume accumulation rate estimates since volume of sediment is what fills the accommodation created by RSLR. To calculate an estimate for total (mineral plus organic) sediment volume accumulation rate along the coast (V_T; m^3/yr) the following equation was used:

$$V_T = A \sum_{i\in pix} V_{a_i}\,. \tag{B7}$$

Volume of organic sediment accumulation rate along the coast (V_{org}; m^3/yr) is calculated as follows:

$$V_{org} = A \sum_{i\in pix} V_{a_i} F_{org_i}\,. \tag{B8}$$

The total mineral volume accumulation rate (V_m; m^3/yr) is calculated as follows:

$$V_m = V_T - V_{org}. \tag{B9}$$

The errors $\left(\delta_{V_x}; \frac{\mathrm{m}^3}{\mathrm{yr}}\right)$ associated with the sediment volume accumulation rates (total, organic, and mineral) are:

$$\delta_{V_T} = V_T \sum_{i \in A} \sqrt{\left(\frac{\delta_{V_{a_i}}}{V_{a_i}}\right)^2}, \tag{B10}$$

$$\delta_{V_{org}} = V_{org} \sum_{i \in A} \sqrt{\left(\frac{\delta_{V_{a_i}}}{V_{a_i}}\right)^2 + \left(\frac{\delta_{F_{org_i}}}{F_{org_i}}\right)^2 + (2V_{a_i} F_{org_i} \sigma_{VF})}, \tag{B11}$$

$$\delta_{V_m} = \sqrt{\left(\delta_{V_T}\right)^2 + \left(\delta_{V_{org}}\right)^2}. \tag{B12}$$

The coast wide trapping efficiency (*TE*; -) is given by:

$$TE = \frac{m_m}{Q_s}. \tag{B13}$$

TE is also calculated for directly and indirectly nourished areas by replacing the numerator with the mineral mass accumulation rate in the directly nourished areas (m_{R_m}) and the mineral mass accumulation rate in the indirectly nourished areas, respectively. The denominator for the indirectly nourished areas is replaced by $Q_s - m_{R_m}$ because the discharge to the coastal ocean necessarily excludes the mineral mass accumulated in the directly nourished wetlands.

The error of the trapping efficiency is only affected by the error on the total sediment mass accumulation rate, since we assume the sediment discharge to be a direct measurement over the study period, therefore assign no uncertainty to the number. The error is calculated as follows:

$$\delta TE = \sqrt{\left(\frac{\delta_{m_m}}{m_m}\right)^2} TE, \tag{B14}$$

where δ*TE* is the estimated error on the trapping efficiency (-).

We then calculated a sediment deficit within the domain by determining the amount of accommodation created along the coast each year using the weighted average subsidence rate and global average SLR rate. In order to have a total net loss of zero cm^2 of land, then:

$$m_N = A \sum_{i \in A} \rho_i RSLR_i, \tag{B15}$$

where m_N is the rate of sediment mass needed (MT/yr) to fill the accommodation created by the RSLR each year. The total error on the mass needed is calculated as follows:

$$\delta_{m_N} = m_N \sqrt{\left(\frac{\delta V_{a_i}}{V_{a_i}}\right)^2 + \left(\frac{\delta RSLR_i}{RSLR_i}\right)^2}, \tag{B16}$$

where δ_{m_N} is the total error on the rate of sediment mass needed (MT/yr) and δ_{RSLR_i} is the error propagated from the standard error on the subsidence rate and the SLR rate, which is a constant 0.0917 cm/yr.

We then compare this mass to the total mass of sediment trapped on the coast each year. Sediment mass deficit is given by:

$$m_D = m_N - m_T, \tag{B17}$$

where m_D is the sediment mass deficit rate (MT/yr). If negative, then there is a sediment mass surplus. The error on the total sediment mass deficit rate ($\delta_{m_D}; \frac{MT}{yr}$) is given by:

$$\delta_{m_D} = \sqrt{\left(\delta_{m_N}\right)^2 + \left(\delta_{m_T}\right)^2}. \quad (B18)$$

A fraction mass sediment deficit is given by:

$$F_{m_D} = \frac{m_D}{m_N}, \quad (B19)$$

where F_{m_D}(-) is the sediment mass deficit or surplus. The error on the fraction mass sediment deficit ($\delta_{F_{m_D}};\ -$) is given by:

$$\delta_{F_{m_D}} = \sqrt{\left(\frac{\delta_{m_D}}{m_D}\right)^2 + \left(\frac{\delta_{m_N}}{m_N}\right)^2}\, F_{m_D}\,. \quad (B20)$$

We normalized this sediment deficit by area to compare the sediment deficit across the coast. The normalized sediment mass deficit is calculated as follows:

$$m_{DA} = \frac{m_D}{A}, \quad (B21)$$

where m_{DA} is the sediment mass deficit rate per area (tonne/km^2/yr). The error on the mass deficit rate per area ($\delta_{m_{DA}}; \frac{tonne}{km^2 yr}$) is:

$$\delta_{m_{DA}} = m_{DA}\sqrt{\left(\frac{\delta m_D}{m_D}\right)^2}\,. \quad (B22)$$

Further, we calculate the estimated sediment mass deficit rate if there was no mass accumulation of organic sediment $\left(m_{D_m}; \frac{MT}{yr}\right)$ and associated error ($\delta m_{D_m}; \frac{MT}{yr}$) along the coast as follows:

$$m_{D_m} = m_N - m_m\,, \quad (B23)$$

$$\delta m_{D_m} = \sqrt{(\delta m_N)^2 + (\delta m_m)^2}\,. \quad (B24)$$

Similarly, we calculate the sediment volume deficit rate and fraction volume deficit. The rate of volume of sediment needed to fill the accommodation created each year is given by:

$$V_N = RSLR * A\,, \quad (B25)$$

where (V_N; m^3/yr) is the rate of volume of sediment needed to fill the accommodation. The error on the rate of the volume of sediment needed ($\delta V_{\mathrm{N}}; \frac{m^3}{yr}$) is given by:

$$\delta V_N = \sqrt{\left(\frac{\delta RSLR}{RSLR}\right)^2}\, V_N\,. \quad (B26)$$

Sediment volume deficit rate is then given by:

$$V_D = V_N - V_T\,, \quad (B27)$$

where V_D is the sediment volume deficit rate (m^3/yr). If negative, then there is a sediment volume surplus. The error on the volume deficit rate ($\delta_{V_D}; \frac{m^3}{yr}$) is given by:

$$\delta_{V_D} = \sqrt{\left(\delta_{V_N}\right)^2 + \left(\delta_{V_T}\right)^2}. \quad (B28)$$

A fraction volume sediment deficit is given by:

$$F_{V_D} = \frac{V_D}{V_N} \ , \quad (B29)$$

where F_{V_D} is the fraction volume sediment deficit (+) or surplus (-). The associated error ($\delta_{F_{V_D}}$; $-$) is given by:

$$\delta_{F_{V_D}} = \sqrt{\left(\frac{\delta_{V_D}}{V_D}\right)^2 + \left(\frac{\delta_{V_N}}{V_N}\right)^2} \, F_{V_D}. \quad (B30)$$

Finally, if there was no organic material accumulating along the coast, the mineral sediment volume deficit rate (V_{D_m}; $\frac{m^3}{yr}$) and associated error (δV_{D_m}; $\frac{m^3}{yr}$) would be:

$$V_{D_m} = V_N - V_m \ , \quad (B31)$$

$$\delta V_{D_m} = \sqrt{\left(\delta_{V_N}\right)^2 + \left(\delta_{V_m}\right)^2} \ . \quad (B32)$$

Lastly, we calculate the fraction of organic material, by mass and volume, for the total land area, the directly and indirectly nourished areas, as well as each basin. We calculate the fraction organic material by mass ($F_{m_{org}}$; $-$) and associated error $\left(\delta F_{m_{org}}; -\right)$ as follows:

$$F_{m_{org}} = \frac{m_{org}}{m_T}, \quad (B33)$$

$$\delta F_{m_{org}} = F_{m_{org}} \sqrt{\left(\frac{\delta m_{org}}{m_{org}}\right)^2 + \left(\frac{\delta m_T}{m_T}\right)^2}. \quad (B34)$$

We also calculate the fraction organic material by volume ($F_{V_{org}}$; $-$) and associated error $\left(\delta F_{V_{org}}; -\right)$ as follows:

$$F_{V_{org}} = \left(\frac{V_{org}}{V_T}\right), \quad (B35)$$

$$\delta F_{V_{org}} = F_{V_{org}} \sqrt{\left(\frac{\delta V_{org}}{V_{org}}\right)^2 + \left(\frac{\delta V_T}{V_T}\right)^2}. \quad (B36)$$

Figure 1.


N
Mississippi River
Atchafalaya River
30°0'0"N
29°0'0"N
Directly Nourished Basins
CRMS Sites
CPRA Hydrologic Basins
Calcasieu/Sabine
Mermentau
Teche/Vermilion
Atchafalaya
Terrebonne
Barataria
Mississippi River Delta ('birds foot')
Breton Sound
Ponchartrain
Pearl
100 km
94°0'0"W
93°0'0"W
92°0'0"W
91°0'0"W
90°0'0"W
89°0'0"W

Figure 2.

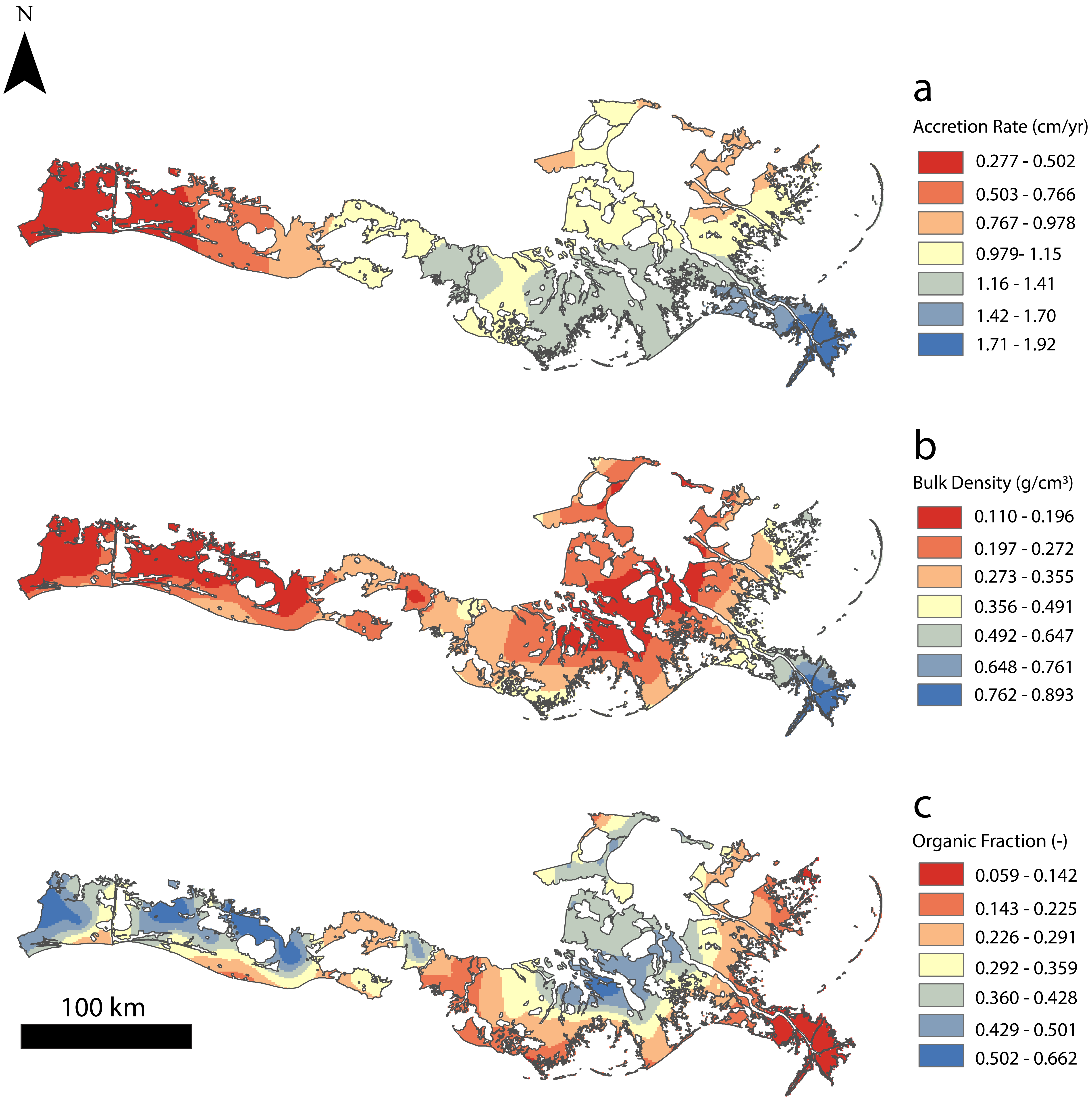
N
a
Accretion Rate (cm/yr)
0.277 - 0.502
0.503 - 0.766
0.767 - 0.978
0.979- 1.15
1.16 - 1.41
1.42 - 1.70
1.71 - 1.92
b
Bulk Density (g/cm³)
0.110 - 0.196
0.197 - 0.272
0.273 - 0.355
0.356 - 0.491
0.492 - 0.647
0.648 - 0.761
0.762 - 0.893
c
Organic Fraction (-)
0.059 - 0.142
0.143 - 0.225
0.226 - 0.291
0.292 - 0.359
0.360 - 0.428
0.429 - 0.501
0.502 - 0.662
100 km

Figure 3.

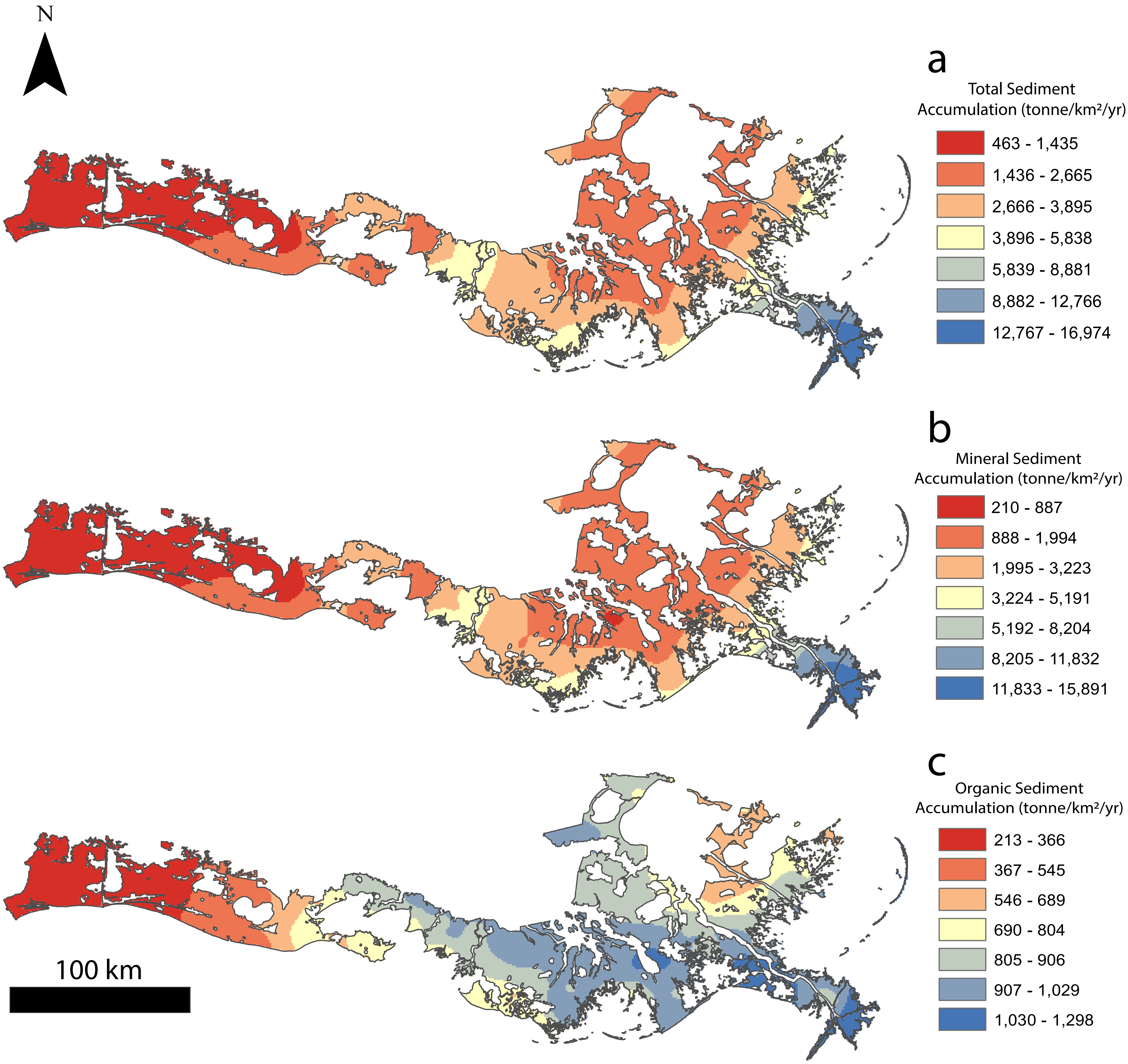
N
a
Total Sediment Accumulation (tonne/km²/yr)
463 - 1,435
1,436 - 2,665
2,666 - 3,895
3,896 - 5,838
5,839 - 8,881
8,882 - 12,766
12,767 - 16,974
b
Mineral Sediment Accumulation (tonne/km²/yr)
210 - 887
888 - 1,994
1,995 - 3,223
3,224 - 5,191
5,192 - 8,204
8,205 - 11,832
11,833 - 15,891
c
Organic Sediment Accumulation (tonne/km²/yr)
213 - 366
367 - 545
546 - 689
690 - 804
805 - 906
907 - 1,029
1,030 - 1,298
100 km

Figure 4.

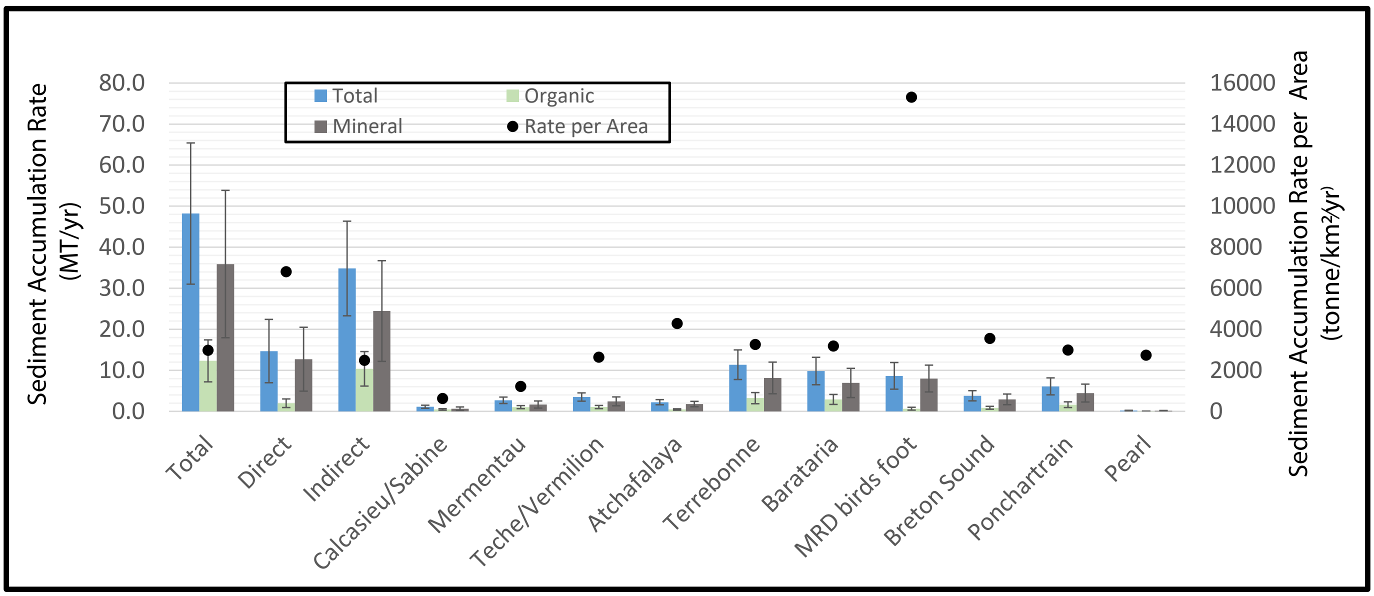

Sediment Accumulation Rate (MT/yr)
80.0
70.0
60.0
50.0
40.0
30.0
20.0
10.0
0.0
Total
Organic
Mineral
Rate per Area
16000
14000
12000
10000
8000
6000
4000
2000
0
Sediment Accumulation Rate per Area (tonne/km²/yr)
Total
Direct
Indirect
Calcasieu/Sabine
Mermentau
Teche/Vermilion
Atchafalaya
Terrebonne
Barataria
MRD birds foot
Breton Sound
Ponchartrain
Pearl

Figure 5.

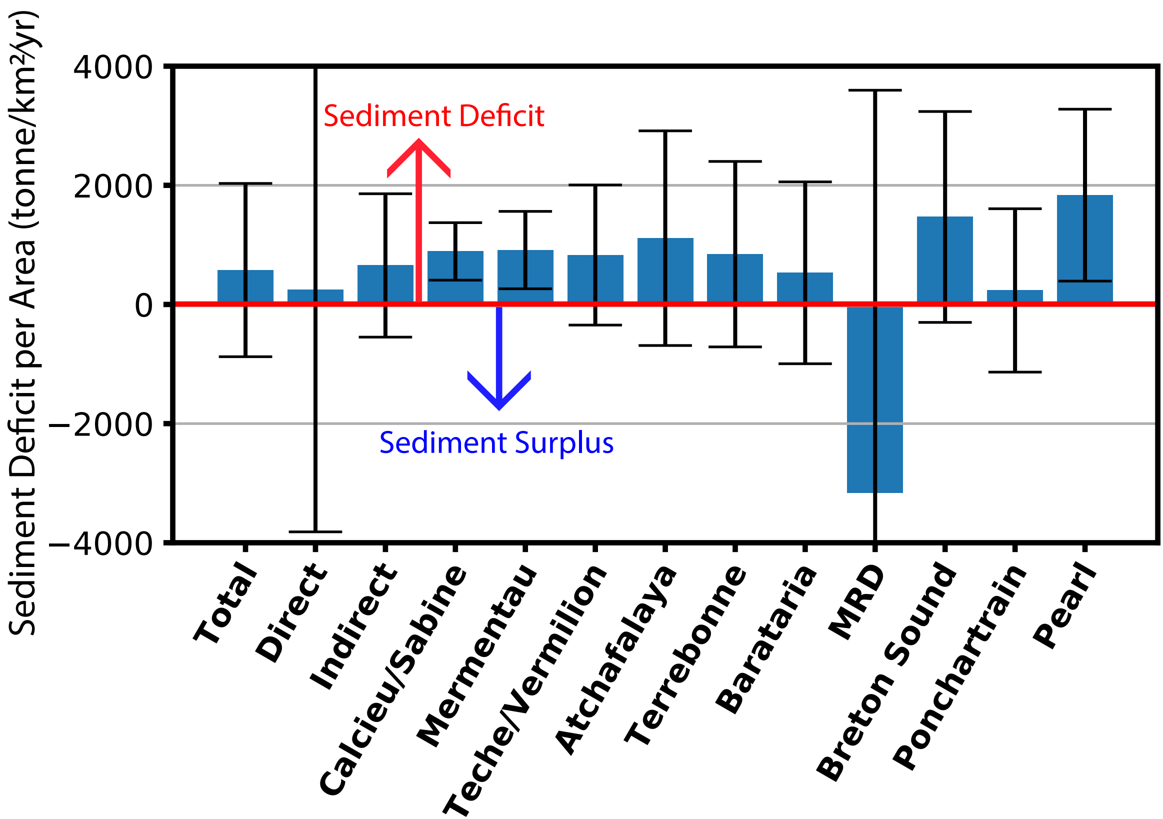

Sediment Deficit per Area (tonne/km²/yr)
4000
2000
0
−2000
−4000
Sediment Deficit
Sediment Surplus
Total
Direct
Indirect
Calcieu/Sabine
Mermentau
Teche/Vermilion
Atchafalaya
Terrebonne
Barataria
MRD
Breton Sound
Ponchartrain
Pearl

Figure 6.

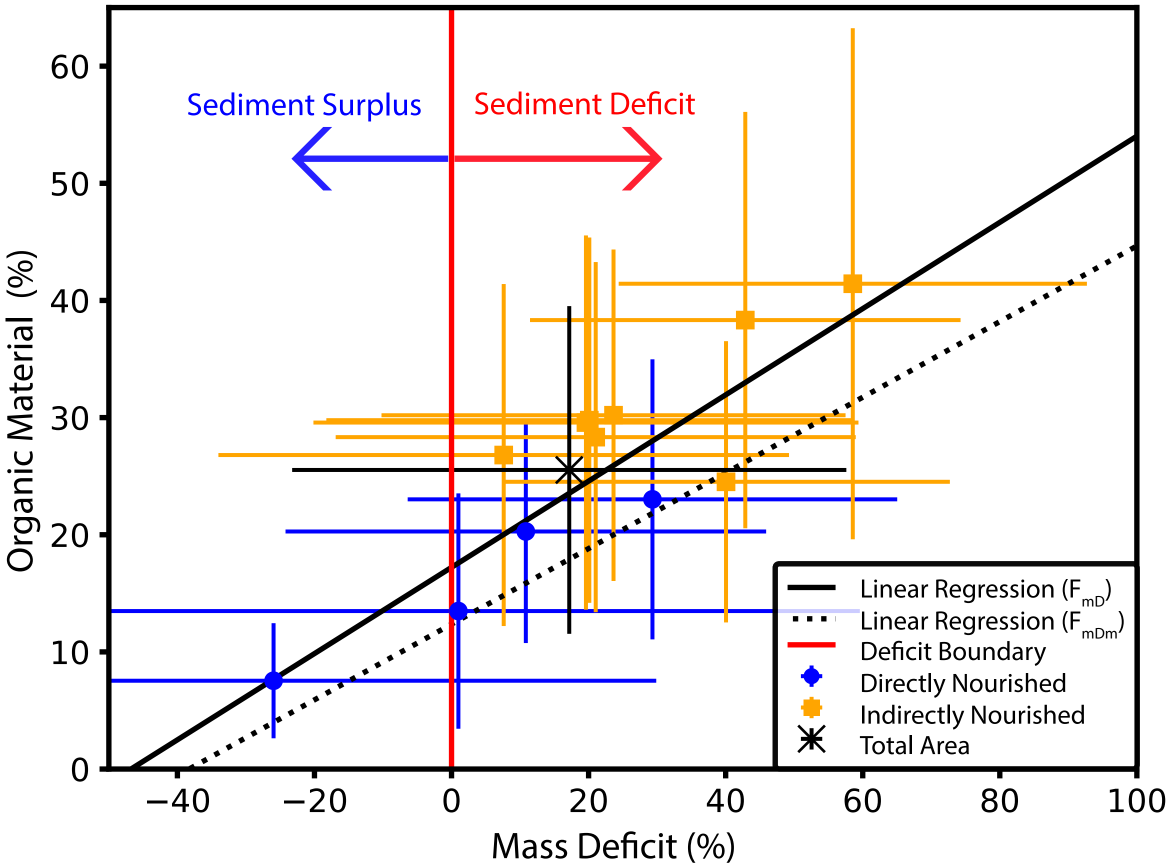

Sediment Surplus
Sediment Deficit
Linear Regression (F_{mD})
Linear Regression (F_{mDm})
Deficit Boundary
Directly Nourished
Indirectly Nourished
Total Area
Organic Material (%)
Mass Deficit (%)
0
10
20
30
40
50
60
−40
−20
0
20
40
60
80
100